Hall Effect, R. E. Prange and S. M. Girvin, Eds. (Springer-Verlag, New York, 1985).
4. B. J. van Wees *et al.*, *Phys. Rev. Lett.* **60**, 848 (1988).
5. For a review, see A. Y. Cho, *Thin Solid Films* **100**, 291 (1983); R. D. Dupuis, *Science* **226**, 623 (1984).
6. For a review, see H. L. Störmer, *Surf. Sci.* **132**, 519 (1983).
7. L. Pfeiffer, K. W. West, H. L. Störmer, K. W. Baldwin, *Appl. Phys. Lett.* **55**, 1888 (1989).
8. For a review, see J. P. Eisenstein and H. L. Stormer, *Science* **248**, 1510 (1990); H. L. Stormer and D. C. Tsui, *ibid.* **220**, 1241 (1983).
9. E. P. Wigner, *Phys. Rev.* **46**, 1002 (1934); for latest developments, see editorial by A. Khurana, *Phys. Today* **43**, 17 (December 1990).
10. For a review, see M. H. Brodsky, *Sci. Am.* **262**, 68 (February 1990).
11. For a review, see L. F. Eastman, *Phys. Today* **39**, 77 (October 1986).
12. For a review, see A. F. J. Levi, R. N. Nottenberg, Y. K. Chen, M. B. Panish, *ibid.* **43**, 58 (February 1990).
13. For a review, see Y. Suematsu, *ibid.* **38**, 32 (May 1985); D. S. Chemla, *ibid.*, p. 57.
14. H. Sakaki, *Jpn. J. Appl. Phys.* **19**, L735 (1980).
15. Y. Arakawa and H. Sakaki, *Appl. Phys. Lett.* **40**, 939 (1982).
16. J. Spector, H. L. Störmer, K. W. Baldwin, L. N. Pfeiffer, K. W. West, *ibid.* **58**, 263 (1991).
17. C. J. B. Ford *et al.*, *J. Phys.* **C21**, 1325 (1988).
18. H. L. Störmer, L. N. Pfeiffer, K. W. West, K. W. Baldwin, paper presented at the International Symposium on Nanostructures and Mesoscopic Systems, Santa Fe, NM, May 1991; L. Pfeiffer, *J. Cryst. Growth* **111**, 333 (1990).
19. E. Kapon, *Appl. Phys. Lett.* **55**, 2715 (1989).
20. P. M. Petroff, A. C. Gossard, W. Wiegmann, *ibid.* **45**, 620 (1984).
21. J. M. Gaines *et al.*, *J. Vac. Sci. Technol.* **B6**, 1378 (1988).
22. T. Fukui and H. Saito, *ibid.*, p. 1373; H. Yamaguchi and Y. Horikoshi, *Jpn. J. Appl. Phys.* **28**, 352 (1989).
23. S. A. Chalmers, H. Kroemer, A. C. Gossard, *Appl. Phys. Lett.* **57**, 1751 (1990).
24. M. S. Miller *et al.*, *J. Cryst. Growth* **111**, 323 (1991).
25. J. Motohisa, M. Tanaka, H. Sakaki, *Appl. Phys. Lett.* **55**, 1214 (1989).
26. K. Tsubaki, Y. Tokura, T. Fukui, H. Saito, N. Susa, *Electron. Lett.* **25**, 728 (1989).
27. T. Fukui, H. Saito, Y. Tokura, *Appl. Phys. Lett.* **55**, 1958 (1989).
28. S. A. Chalmers *et al.*, *ibid.*, p. 2491.
29. P. I. Cohen and P. R. Pukite, *J. Vac. Sci. Technol.* **A5**, 2027 (1987).
30. S. A. Chalmers, A. C. Gossard, P. M. Petroff, J. M. Gaines, H. Kroemer, *ibid.* **B7**, 1357 (1989).
31. P. R. Pukite, C. S. Lent, P. I. Cohen, *Surf. Sci.* **161**, 39 (1985).
32. J. H. Neave, P. J. Dobson, B. A. Joyce, J. Zhang, *Appl. Phys. Lett.* **47**, 100 (1985).
33. F. Briones, D. Golmayo, L. Gonzalez, A. Ruiz, *J. Cryst. Growth* **81**, 19 (1987); Y. Horikoshi, M. Kawashima, H. Yamaguchi, *Jpn. J. Appl. Phys.* **27**, 169 (1988).
34. S. A. Chalmers, A. C. Gossard, P. M. Petroff, H. Kroemer, *J. Vac. Sci. Technol.* **B8**, 431 (1990).
35. V. Celli and N. D. Mermin, *Phys. Rev.* **140**, A839 (1965).
36. The suggestion was made by A. C. Gossard and B. I. Halperin: see B. I. Halperin, *Jpn. J. Appl. Phys.* **26** (Suppl. 26-3), 1913 (1987).
37. M. Sundaram, A. C. Gossard, J. H. English, R. M. Westervelt, *Superlattices Microstruct.* **4**, 683 (1988).
38. These calculations solve both Poisson's equation and the Schrödinger wave equation with appropriate boundary conditions: see A. J. Rimberg and R. M. Westervelt, *Phys. Rev. B* **40**, 3970 (1989); T. Sajoto, J. Jo, H. P. Wei, M. Santos, M. Shayegan, *J. Vac. Sci. Technol.* **B7**, 311 (1989); M. P. Stopa and S. DasSarma, *Phys. Rev. B* **40**, 10048 (1989); A. Wixforth, M. Sundaram, K. Ensslin, J. H. English, A. C. Gossard, *Appl. Phys. Lett.* **56**, 454 (1990).
39. A. C. Gossard, *IEEE J. Quant. Electron.* **22**, 1649 (1986).
40. M. Sundaram, A. Wixforth, R. S. Geels, A. C. Gossard, J. H. English, *J. Vac. Sci. Technol.* **B9**, 1524 (1991).
41. M. Sundaram, A. C. Gossard, P. O. Holtz, *J. Appl. Phys.* **69**, 2375 (1991).
42. M. Shayegan, J. Jo, W. Suen, M. Santos, V. J. Goldman, *Phys. Rev. Lett.* **65**, 2916 (1990).
43. See, for example, P. F. Hopkins *et al.*, *Appl. Phys. Lett.* **57**, 2823 (1990).
44. E. G. Gwinn *et al.*, *Phys. Rev. B* **39**, 6260 (1989); T. Sajoto, J. Jo, M. Santos, M. Shayegan, *Appl. Phys. Lett.* **55**, 1430 (1989); K. Ensslin, M. Sundaram, A. Wixforth, J. H. English, A. C. Gossard, *Phys. Rev. B* **43**, 9988 (1991).
45. M. Sundaram and A. C. Gossard, in preparation.
46. K. Karraï, H. D. Drew, M. W. Lee, M. Shayegan, *Phys. Rev. B* **39**, 1426 (1989); K. Karraï, X. Ying, H. D. Drew, M. Shayegan, *ibid.* **40**, 12020 (1989).
47. A. Wixforth, M. Sundaram, K. Ensslin, J. H. English, A. C. Gossard, *ibid.* **43**, 10000 (1991).
48. L. Brey, N. F. Johnson, B. I. Halperin, *ibid.* **40**, 647 (1989).
49. W. W. Bewley *et al.*, in preparation.
50. M. Sherwin, in preparation.
51. J. Jo *et al.*, *Appl. Phys. Lett.* **57**, 2130 (1990); A. J. Rimberg *et al.*, paper presented at the International Symposium on Nanostructures and Mesoscopic Systems, Santa Fe, NM, May 1991.
52. J. Maserjian and A. C. Gossard, patent pending.
53. W. Walukiewicz, M. Sundaram, P. F. Hopkins, A. C. Gossard, R. M. Westervelt, in *Proceedings of the MRS Fall Meeting*, Boston, MA, 1990 (Materials Research Society, Pittsburgh, 1990).
54. We thank the following colleagues for discussions on matters pertaining to this article: P. M. Petroff, H. Kroemer, J. H. English, H. Weman, M. Miller, A. Wixforth, K. Ensslin, E. G. Gwinn, R. M. Westervelt, M. S. Sherwin, B. I. Halperin, A. J. Rimberg, and M. P. Stopa. Our thanks also to J. C. Yi for calculating and preparing Fig. 5, to S. Gidir and K. Campman for critical readings of the manuscript, and to D. J. McLarin for her skillful translation of some of the authors' ideas into lucid figures.

Microfabrication Techniques for Integrated Sensors and Microsystems

K. D. Wise and K. Najafi

Integrated sensors and actuators are rapidly evolving to provide an important link between very large scale integrated circuits and nonelectronic monitoring and control applications ranging from biomedicine to automated manufacturing. As they continue to expand, entire microsystems merging electrical, mechanical, thermal, optical, magnetic, and perhaps chemical components should be possible on a common substrate.

The dramatic progress made by microelectronics over the past 30 years is obvious today in nearly all aspects of society. The number of transistors that can be successfully integrated on a single silicon chip is now over a million, and by the end of this decade that number is expected to increase another thousandfold. This progress will make very sophisticated control systems possible at low cost; however, the application of such systems in health care, biotechnology, industrial automation, automotive systems (including smart highways), and many consumer products will depend on the availability of low-cost, high-performance sensors and actuators with which to interface this control circuitry to a nonelectronic world. In response to increasing pressure from such system needs, during the past 30 years there has been an expanding effort toward sensor development based on the use of technologies similar to those used for integrated circuits.

The late 1960s saw the first efforts at adapting microfabrication techniques to the creation of miniature silicon sensors. After early temperature and pressure sensors, optical detector arrays were probably the first such devices to find their way into production, and today these devices are among the largest chips fabricated by the semiconductor industry, promising to revolutionize photography at

The authors are with the Center for Integrated Sensors and Circuits, The University of Michigan, Ann Arbor, MI 48109.

all levels. Progress has been rapid, in part, because fabrication requires relatively few processes or packaging techniques beyond those used for integrated circuits themselves. Pressure sensors, in contrast, have always required special selective etching (micromachining) and packaging techniques in order to be practical in silicon. In the 1970s considerable progress was made in the development of micromachining techniques for such devices with the emergence of impurity-based etch-stops, which took silicon sensors out of the laboratory and into volume production. The automotive industry was a primary impetus in these developments. By the late 1980s, surface micromachining had also emerged, making possible a variety of new resonant sensors and microactuators, and circuits were being successfully merged with microsensors and actuators to ease signal-to-noise and packaging problems. Flow meters and accelerometers were joining pressure sensors as high-volume production devices, and many other devices were under development.

With the addition of microactuators to the expanding arsenal of microsensors and interface circuitry, many of the elements for the creation of complete integrated microsystems appear to be in place (*1*). Accordingly, there have been many proposals for the creation of such systems, with applications ranging from tiny microrobots for security and medical applications to sophisticated positioning systems for assembly tasks at the submillimeter level. It is certain that today we have only scratched the surface in defining important applications for such microsystems, and, if we are successful, the 1990s should see the practical realization of structures merging mechanical, electrical, thermal, magnetic, optical, and perhaps chemical components, all on a common substrate. These components will extend from monolithic subsystems having micrometer and submicrometer features to multichip hybrid structures at the millimeter level, where advanced assembly and packaging techniques will be particularly important. Many groups around the world are intensively developing a variety of microsensors, microactuators, and new microfabrication technologies for a number of applications. This article will focus primarily on recent developments in silicon-based microstructures, where much of the recent research has concentrated.

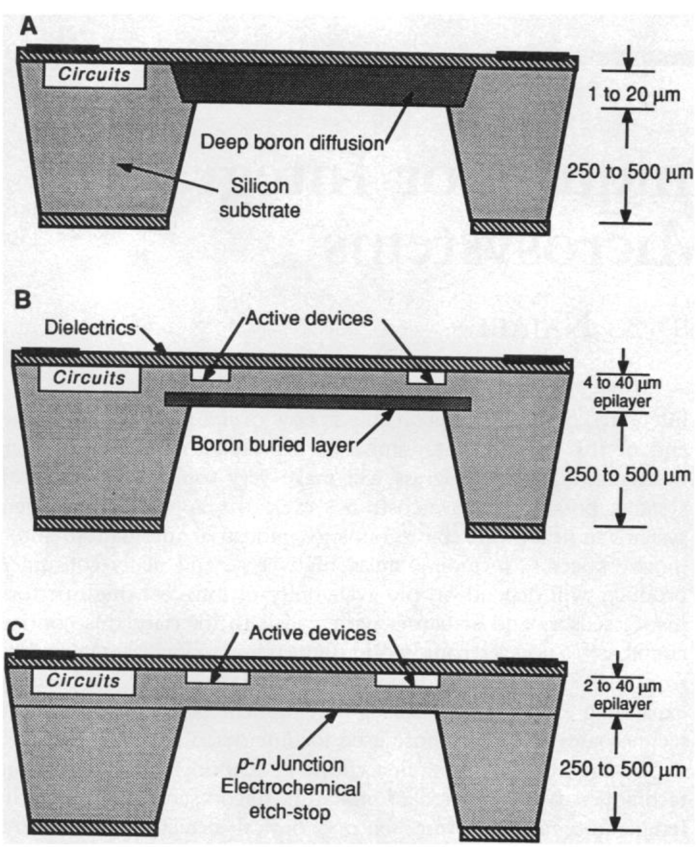

Fig. 1. Typical cross section of a bulk micromachined silicon wafer with various methods for etch-stop formation. (**A**) Diffused boron etch-stop; (**B**) boron etch-stop as a buried layer; (**C**) electrochemical etch-stop.

Fabrication Technologies and Emerging Sensors

Bulk micromachining. What we know today as micromachining was born during the 1960s as researchers at Bell Telephone Laboratories struggled to develop precise silicon etching techniques for beam-lead air-isolated integrated circuits (*2*). Early work was based on isotropic etchants, which were easily used but difficult to control. Anisotropic etchants for silicon (*3*), most notably potassium hydroxide (KOH), ethylene diamine pyrocatechol (EDP), and hydrazine, were developed in the late 1960s and are the basis for most micromachining today. These chemicals are more easily masked and less agitation-sensitive than their isotropic counterparts, attacking the <100> crystallographic direction in silicon much faster than the <111> direction. Thus, highly directional and very reproducible etching is possible.

For many sensors, the microstructure required is in the form of a diaphragm or beam (Fig. 1). With the use of photolithography, an etch mask (typically silicon dioxide or silicon nitride) is defined on the back of the wafer in alignment with patterns on the front surface. The wafer bulk is selectively etched from the back as the final step in the wafer process to form the microstructure while die separation is performed simultaneously. However, because most beams or diaphragms of interest are of the order of 1 to 20 μm thick, there is a serious problem to be overcome in allowing the batch formation of microstructures controlled to within a fraction of a micrometer from 400- to 600-μm-thick wafers.

The existence of impurity-based etch-stops in silicon (*4*) has allowed micromachining to become a high-yield production process during the past decade. The first and most widely used etch-stop technique (Fig. 1A) is based on the fact that anisotropic etchants, especially EDP, do not attack heavily boron-doped ($p+$) silicon.

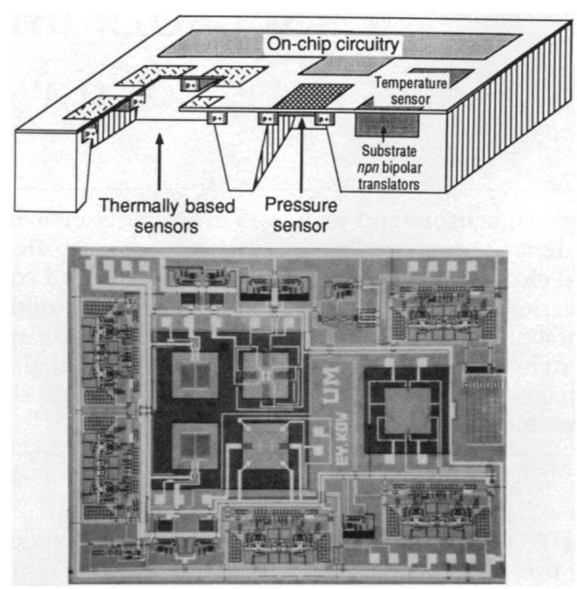

Fig. 2. Structure and top view of a monolithic mass flow sensor containing transducers for gas flow rate, direction, type, pressure, and temperature. The chip measures 3.5 mm by 5 mm in 3-μm CMOS technology with 0.5-mm square windows used for the transducers.

Thus, a simple boron diffusion introduced from the front of the wafer can be used to create beams and diaphragms. Layers of $p+$ silicon having thicknesses from 1 to about 20 μm can be formed with this process. Because the boron-doped silicon is in tensile stress, the microstructures are flat and do not buckle; however, because the silicon must be doped above 5×10^{19} cm^{-3} to achieve an etch-stop, it is not possible to fabricate circuit elements within this material. To overcome this problem, more lightly doped silicon epitaxial layers have been used over $p+$ buried layers (Fig. 1B); however, epitaxial quality is compromised to some extent by the high substrate doping. If instead a voltage can be applied across the sample during the etch, a lightly doped epitaxial layer of one conductivity type (for example, *n*-type) on a lightly doped substrate of the opposite type (for example, *p*-type) can be used to form an etch-stop at the episubstrate *p-n* junction. This electrochemical process (*5*) permits the formation of high-quality devices but requires the added complication of bias during the etch (Fig. 1C).

A bulk-micromachined monolithic mass flow meter was recently developed at the University of Michigan (*6*) (Fig. 2). This device supports its various transducers by means of stress-compensated dielectric windows below which the silicon has been removed by means of an etch from the back of the wafer. These windows provide thermal isolation in the realization of sensors for gas flow velocity, flow direction, and gas type. A polysilicon heater and a thin-film temperature transducer on each window maintain constant temperature there in the face of energy transfer to the moving gas stream, and the measurement of the power associated with convective cooling allows a determination of flow rate. A separately etched well is used to form a piezoresistive polysilicon-bridge pressure sensor. The thin diaphragm here is composed of 2 μm of boron-doped silicon overlaid by stress-compensated silicon dioxide–silicon nitride dielectrics. On-chip complementary metal-oxide semiconductor (CMOS) circuitry is used to provide amplified multiplexed transducer outputs, set the operating window temperatures, implement self-test circuitry, and realize a band-gap absolute-temperature sensor. Thus, the chip measures all of the parameters needed for the computation of mass flow, provided that the flow channel dimensions are known. The device demonstrates a generic sensor structure, providing a flow response from 1 cm s^{-1} to over 5 m s^{-1}, a flow direction resolution of 5°, a pressure range of 0 to 800 $\pm$ 1 torr, and a temperature range from $-40°$ to $+120$°C.

Bulk micromachining has been used for most of the integrated sensors produced thus far by the industry; however, the long etch time (several hours) required to etch through the silicon substrate from the back is an increasingly objectionable feature of this process in some applications. This problem is overcome in two relatively new approaches: bulk dissolved-wafer processes (7) and surface micromachining (*8*). In dissolved-wafer processes, the wafer is processed to form the required etch-stops and active devices and is then bonded facedown to a second wafer of glass or silicon by one of the processes to be mentioned below. The first wafer is then dissolved with an unmasked etch from the back to leave the desired microstructures attached to the bottom wafer. If free (nonsupported) structures are desired, the second wafer can simply be eliminated. Because the wafer dissolution etch can be done in two steps (a fast isotropic etch followed by a slower anisotropic etch for the last 50 to 100 μm), the processing is all single-sided and the need for a slow etch through the entire wafer is avoided. When glass is used as the second wafer, wafer-to-wafer alignment is much simplified and stray capacitance is minimized. Active circuitry can be attached to the glass to form a multichip hybrid. When silicon is used as the lower wafer, circuitry can be embedded in it to form the active system.

Dissolved-wafer processing to form free integrated sensors has been used in the development of advanced neuroelectronic interfaces currently under way at the University of Michigan. These structures are intended both for the study of signal processing techniques in biological neural nets and for application in advanced neural prostheses (*9, 10*). A multichannel micromachined recording array has been fabricated for such applications (Fig. 3). The silicon probe substrate is defined with the use of a deep boron-diffused etch-stop, with circuitry formed in a lightly doped portion of the substrate near the rear of the probe. Recording sites formed from inlaid gold or iridium are located along the shank and are connected to circuitry on the back of the probe with interconnects that are insulated above and below by stress-relieved composite films of silicon dioxide and silicon nitride. These probes are capable of extracellular recording from many cells in the brain simultaneously on a spatially distributed basis and allow a much more detailed look at neural circuits than has been possible in the past. For the most recent version of such devices (*11*), on-chip CMOS circuitry allows the optimization of recording site placements by the selection of 8 of 32 available sites for monitoring and amplification, effectively realizing electronic site positioning. Each of the on-chip amplifiers occupies only 0.06 mm^2 in 3-μm CMOS technology, provides a per-channel gain of 300, and limits the bandwidth of the recorded signals to 10 Hz to 10 kHz while requiring no off-chip components and allowing a three-lead interface to the external world. The devices are completely self-testing. Only the *p*-well implant dose in the circuit portion of the overall process is modified as it is merged with the sensor process. The *p*-well drive is performed simultaneously with etch-stop formation. The process is stable, single-sided, and high-yield. A series of stimulating probes is also under development on the basis of this same technology.

Packaging is a critical element in the creation of long-term assemblies of these probes, as is the development of microassembly techniques to permit three-dimensional arrays of probes capable of monitoring the activity of neurons throughout a volume of tissue. With the same technology, the interconnect leads required to connect the probe to a percutaneous connectors can be formed and can even be built into the probe substrate. Multilead multistrand silicon-substrate ribbon cables have been formed in which each conductor lead is insulated and surrounded by a conducting shield to form a multilead coax (*12*). These lead structures are 5 μm thick, extremely flexible, and up to 5 cm long. They exhibit minimal tethering forces on the implanted probes and have allowed significant progress on the difficult problem of connecting to long-term implanted microsensors in the body. The cables are also of potential interest in other applications where signals must be interfaced to

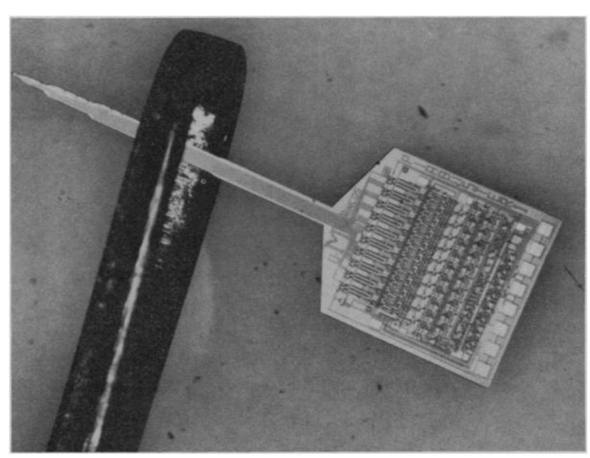

Fig. 3. A multichannel multiplexed intracortical microprobe produced by micromachining. The overall probe is 4.7 mm long and is shown passing through the eye of a needle.

movable microstructures. In an alternative leadless design for cortical use, a three-dimensional multiprobe (*13*) assembly has been constructed in which several multishank probes are assembled in a silicon micromachined platform. Batch feedthroughs interconnect circuitry on the probes to additional circuitry on the platform (Fig. 4). Such assembly techniques will be a vital part of many future microsystems.

Wafer bonding processes. Wafer-to-wafer bonding techniques (*14*) are useful as companions or possible alternatives to micromachining. These have been referred to in connection with the dissolved-wafer bulk processes above. The first of these techniques is electrostatic (anodic) bonding of silicon to glass (*15*). This process was developed in the 1960s, and the first sensor applications took place in the 1970s. The silicon sensor wafer is placed in contact with a glass wafer whose thermal expansion coefficient closely matches that of silicon. Corning code 7740 glass (Pyrex) is usually used for this purpose. The assembly is raised to a temperature of typically 400° to 600°C, and a voltage of 400 to 1000 V is applied (silicon-positive). Most of the applied voltage is dropped across the silicon-glass interface, inducing a permanent irreversible fusion bond that is stronger than either of the materials individually. Such bonds have been used for a wide variety of microstructures. The electrostatic bond can also be used to join silicon to silicon if an intermediate layer of glass is used. Typically, 2- to 4-μm-thick layers of sputtered borosilicate glass have been used for this purpose. Although these structures have been especially effective for stress-relieved die-attach packaging, long sputtering times associated with the glass deposition are required.

Silicon-to-silicon fusion bonds (*16*) can be produced at the wafer level if two silicon wafers are placed in contact and are heated to temperatures in excess of 1000°C. Such bonds can be used to produce a variety of complex microstructures impossible with bulk or surface micromachining alone; however, the high bonding temperatures and the need for precision wafer alignment are difficulties as is the need to obtain high coverage of the bonded areas. In the electrostatic bond, the applied field provides a powerful local force drawing the wafers together. With fusion bonding, this local force is absent and area coverage is usually lower. With both bonding techniques, the surfaces to be bonded must be highly planar because the bonds produce little actual material flow. In the electrostatic bond, planarity must be to within 30 to 50 nm in order to ensure a hermetic seal.

A pressure-based approach to flow measurement (*17*) has been developed with a four-mask dissolved-wafer process (Fig. 5). A microchannel for gas flow is micromachined into silicon and combined with a silicon capacitive pressure sensor to realize a chip that is orders of magnitude more sensitive than commercial flow devices. Gas enters and exits the flow channel through holes in the glass substrate, and the pressure generated by gas flow through the channel is applied across the pressure sensor diaphragm. The device measures pressures from 1 mtorr to over 100 torr, with hysteresis, creep, and fatigue all consistent with a measurement resolution of 16 bits. The equivalent flow resolution is 10^{-8} standard cubic centimeter per minute. In addition, because the device is sensitive to relatively low pressures, electrostatically generated forces can be used to make the sensor self-testing (*18*). Thus, the device becomes a sort of microelectromechanical system unto itself, with the actuator used for sensor self-test. Accelerometers are also emerging that incorporate these characteristics. As has been the case in data converters, silicon sensors, at least for mechanical variables, are rapidly growing in performance and may soon displace individually assembled precision devices even at the high end of the applications spectrum. Resonant beam sensors (*19*) and bulk static devices may both compete in this arena.

Surface micromachining. A microfabrication technique that has attracted great attention recently is surface micromachining. This technique has been used to fabricate a number of microstructures, including resonant microsensors and electrostatically driven micromotors. Surface micromachining can utilize any of a number of deposited thin films available in integrated circuit technology,

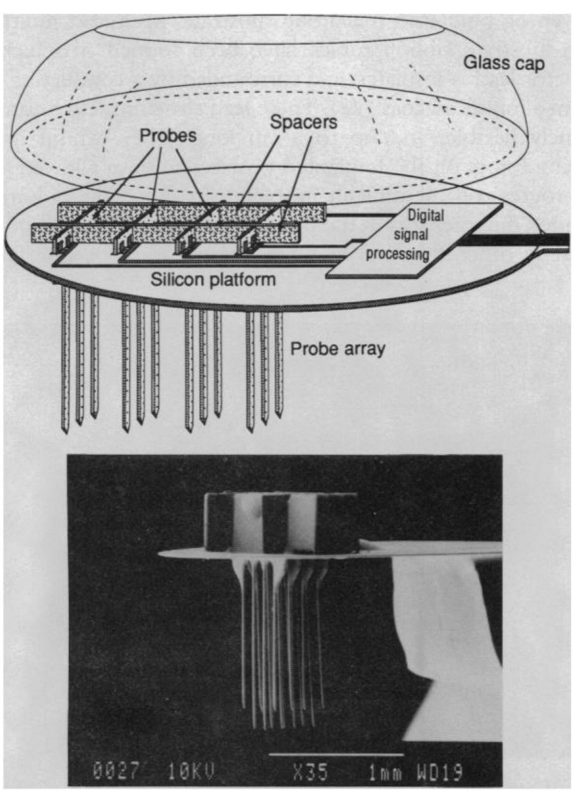

Fig. 4. A three-dimensional microsystem consisting of multiple neural probes assembled in a micromachined silicon platform.

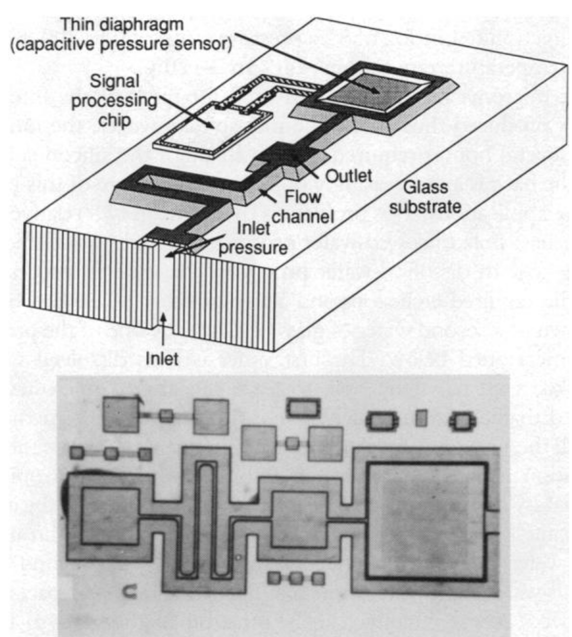

Fig. 5. Diagram and photograph of an ultrasensitive silicon microflow meter. The flow range using the on-chip flow channel is from 10^{-8} to 10^{-3} standard cubic centimeter per minute, with a pressure range from 1 mtorr to over 100 torr. The die size is 3 mm by 9 mm.

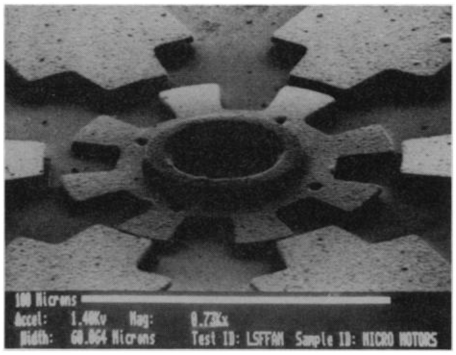

Fig. 6. A six-stator polysilicon micromotor developed recently at the University of California, Berkeley, using surface micromachining. [Photo courtesy of R. S. Muller, University of California, Berkeley]

including polycrystalline silicon (polysilicon), silicon nitride, and a number of metallic thin films. To fabricate structures by surface micromachining, a sacrificial film (typically silicon dioxide) is first deposited and patterned on the silicon wafer. The wafer may have undergone other previous processing and may already be coated with silicon nitride. The film for the desired microstructure is next deposited and patterned, and the sacrificial layer is then etched away, undercutting the microstructure and leaving it freely suspended, anchored only where it reached beyond the patterned sacrificial layer to contact the substrate.

The earliest attempt at using surface micromachining for the fabrication of micromechanical devices was by Nathanson *et al.* (*20*), at Westinghouse in the late 1960s. They fabricated a metal thin-film tuning fork (cantilever beam) and demonstrated its electrostatic control. However, it was not until the early 1980s that the real capabilities of surface micromachining were demonstrated by Howe and Muller, who fabricated a resonant vapor sensor based on a free-standing polysilicon bridge structure (*21*) at the University of California, Berkeley. This device demonstrated the potential of surface micromachining techniques and of polysilicon thin-film structures for the fabrication of micromechanical systems. A similar process developed by Guckel and Burns at the University of Wisconsin produced vacuum-sealed diaphragms for use as pressure sensors (*22*). Since then, a number of microelectromechanical devices have been fabricated with polysilicon thin films. These early efforts also led to the development of rotary micromotors by a number of groups, including Gabriel and co-workers of AT&T Bell Laboratories (*23*), Mehregany of Case Western Reserve University and Senturia of MIT and their colleagues (*24*), and Fan, Tai, and Muller of Berkeley (*25*). The rotary micromotors (Fig. 6) are driven electrostatically (that is, with attractive forces generated by applying a voltage across a narrow gap separating the rotor from a fixed stator) and measure less than 100 μm in diameter; the micromotors have been operated at speeds exceeding 20,000 rpm, although friction and wear remain challenges for devices that must operate continuously. Comb-driven lateral micromechanical devices are also potentially useful because it is easier to couple to them and they exhibit a more linear response.

The rapid development of surface micromachined micromechanical devices has been in large part due to two factors: (i) the development and utilization of reactive ion-etching techniques to precisely define features and spacings in the deposited thin films; and (more importantly) (ii) progress in improved understanding of the mechanical properties of the thin films (particularly polysilicon) that are so crucial in forming devices that have freely moving parts. Although most of these structures have used polysilicon as the mechanical material, other thin films, including polymers and metals, have also been used in the fabrication of such systems. Chen and MacDonald of Cornell (*26*) have used thin films of tungsten to fabricate microtweezers and rotary micromotors similar in function to those formed in polysilicon.

Resonant microsensors can be easily fabricated with surface micromachining technology, and a variety of accelerometers and pressure sensors are currently under development for automotive and consumer applications. The ability to fabricate sensors and actuators with built-in self-test and autocalibration capabilities is a desirable feature for systems in which long-term reliability and stability are of critical importance. Surface micromachined structures are already finding important applications in these areas.

In spite of its many desirable features, surface micromachining as it is normally used is limited to the fabrication of devices having low profiles and thicknesses in the range of a few micrometers. This limitation is dictated by the deposition techniques used for the thin films in the microstructures. However, many micromechanical devices, especially microactuators, require structures that have thicknesses of tens of micrometers or more in order to improve the rigidity of the devices, allow reliable coupling to them, and generate sufficient forces at the micro- and milliscales. The dissolved-wafer technology discussed earlier allows the fabrication of microstructures with thicknesses as great as 20 μm and in this sense provides an alternative to surface micromachining, particularly when combined with dry etching. Although nearly all micromachining for sensors in the past has used wet chemistry, increasing use is now being made of dry-etching processes in which the reactive ions are generated in a vacuum-based plasma system. Such etching makes it possible to etch materials such as silicon nitride, which are difficult to etch with wet chemistries, and the etch can be highly directional when the isotropic properties of a straight plasma etch are combined with the directional properties associated with physical bombard-

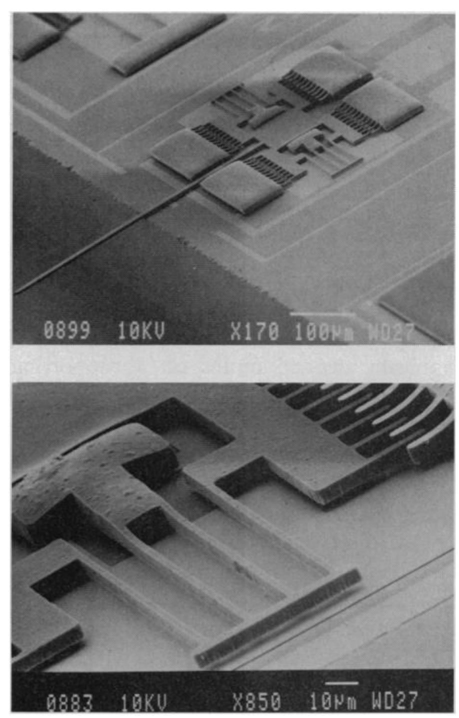

Fig. 7. Scanning electron microscope views of a laterally driven microprobe for use in a scanning thermal profilometer. The probe is produced by means of a dissolved-wafer process, with boron diffusions defining the bulk silicon microstructures and reactive ion etching used to provide accurate lateral control of dimensions. Forces generated electrostatically across the comb structures shown are used to scan the structure.

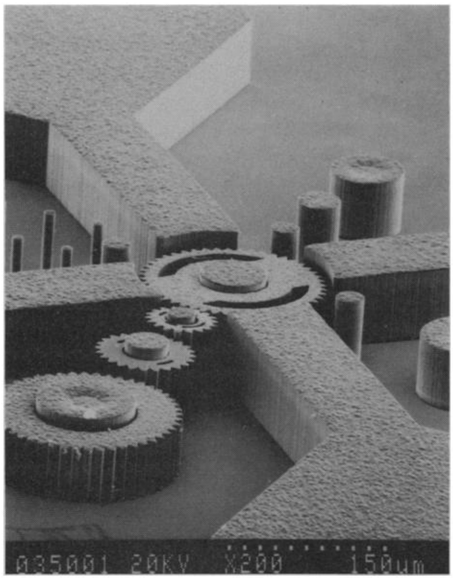

Fig. 8. Scanning electron microscope view of an assembled magnetically driven micromotor fabricated by the sacrificial LIGA process. The rotor diameter is 150 μm, and the gears have diameters of 77, 100, and 150 μm. [Photo courtesy of H. Guckel, University of Wisconsin]

ment as, for example, in reactive ion etching (*27*). It is likely that some of the most demanding requirements for the dry etching of silicon will come from the desire to create silicon sensors and actuators with deep micrometer and submicrometer features.

A laterally driven microprobe tip for use in a scanning thermal profilometer (Fig. 7) is being developed at the University of Michigan (*28*). In its preparation a bulk dissolved-wafer process is used in combination with reactive ion etching. The boron-doped silicon is ~6 μm thick and rides about 2 μm above the glass wafer. Structures as thick as 20 μm have been fabricated with the use of the same technology by Suzuki at NEC (*29*). An attractive feature of this process for microactuators is the ease with which overhung structures can be fabricated. The microprobe in Fig. 7 extends a distance of 300 μm over the edge of the glass substrate.

Electroforming processes (LIGA). Microstructures with very high aspect ratio (thickness to width) can be fabricated with x-ray lithography and electroforming processes. Originally developed in Germany (where its acronym "LIGA" was derived) and significantly extended at the University of Wisconsin, this approach takes advantage of the ability to electroplate metallic films through thick photolithographically defined molds on a supporting substrate. Very thick photosensitive polymers such as polymethylmethacrylate are spun onto wafers and exposed to high-energy x-rays through appropriate masks. The exposed regions are then dissolved in developers, and the remaining material acts as a mold for the final microstructure. Because of the short wavelength of the x-rays and the thickness of the photosensitive polymers (thicknesses approaching 300 μm), the molds can achieve aspect ratios approaching 300:1. Metal films are then electroplated to fill the mold in the areas where the polymer mask has been removed. When the mold material is subsequently removed, the metallic microstructure is left on the wafer surface where it can be freed if desired by surface micromachining. Rotary micromotors, laterally driven microstructures, gear trains, and a variety of other devices have been fabricated (*30, 31*). A SLIGA (sacrificial LIGA) micromotor (Fig. 8) has been developed by Guckel *et al.* at the University of Wisconsin (*32*). Because nickel is usually used as the plating material for these microstructures, electromagnetically generated forces can be used to drive them; the micromotor shown has been operated magnetically. The main advantages of this technology are its large thickness and aspect ratio, the ability to generate large forces and torques, and the ability to fabricate truly three-dimensional devices that cannot be fabricated with any other technique. The technology appears capable of producing complex drive mechanisms and machines with precise dimensions, for example, for applications in driving miniature magnetic storage disks and in other areas requiring large elements with tight tolerances. The chief disadvantage of this technology is that an appropriate source of x-ray radiation is required. Electroplated microstructures with thicknesses up to about 40 μm can also be fabricated with ultraviolet lithography (*33*). This eliminates the need for the x-ray source and makes the process more widely available at the expense of more limited layer thicknesses and reduced aspect ratios.

System aspects. As a final comment, the system aspects of these devices should be mentioned. There are currently a number of important efforts under way to establish interface standards for next-generation "smart" sensors. At Michigan, all devices now being developed conform to a standard interface structure (*1*) that allows the devices to work with a very large scale integration interface chip in the sensing node to implement digital compensation, self-testing, and bus compatibility at the system level. The above microflow meter is currently running on a reactive ion etcher in our laboratory where it is assisting in the development of advanced dry micromachining processes for both sensors and large-scale integrated circuits.

In summary, for an expanding number of sensors, high-yield batch-processing techniques have been established that are consistent with on-chip circuitry. The circuit processes often require little or no modification from standard techniques and hence are process-foundry, and perhaps circuit-foundry, compatible. Integrated lead structures have been developed that allow minimal tethering to free-standing microchips and to microelectromechanical assemblies. The first steps toward three-dimensional microsystems have been taken, and the generic nature of some microstructures has been demonstrated. Finally, some sensors are evolving to a high level of accuracy, making digital compensation, self-testing, and bus interfacing attractive and attainable features.

Future Technology Needs

Although much progress has been made in some classes of sensors, a host of challenging problems remain for other devices, and for actuators and microsystems development is in its infancy. Many such systems are not likely to be monolithic at all but will be multichip hybrids on silicon or insulating substrates. Much improved understanding, characterization, and control over the mechanical properties of the films used in the fabrication of microstructures is badly needed. Such issues as the control of stress and strain in various thin films and the removal of stress by a variety of annealing techniques will have to be confronted for both existing and new microfabrication technologies. With this resulting knowledge base, we can hope to design, simulate, and successfully fabricate new and more complicated microsystems that will perform as intended. Improved packaging and microassembly techniques are also badly needed and have as yet scarcely been addressed. Chemical sensors are not yet highly developed, and we have not adequately addressed the integration of optical sources and detectors as part of overall microsystem development beyond limited efforts at fiberoptic repeater systems.

In the area of microactuators, we badly need drive mechanisms capable of producing high force and high displacement simultaneously. The planar nature of silicon technology is a major limitation for many future systems, including microvalves and pumps. Batch wafer-to-wafer process technologies, microstructures, and assembly techniques are needed that will permit stacked three-dimensional systems to be formed using a set of robust construction primitives, including support pillars, lead columns, mechanical elements, and signal-processing platforms. In addition, robust workstation-based simulators are badly needed, both as a means for the rapid design of microsystems and also to allow models to be used to improve our fundamental understanding of them. These stations should include databases incorporating process-material data, gateways to commercial finite-element code, and links to solid-state process-device-circuit simulators. There are efforts in these directions (*34, 35*), but much more needs to be done. Thus, although we have made substantial progress in some areas of sensors, the challenges before us are broader still and must be the focus for major efforts throughout the decade of the 1990s. Solving these problems will require the focusing of multidisciplinary teams from engineering, chemistry, physics, business, and the life sciences, both in universities and in industry.

It is encouraging that important applications for microsystems are emerging, including uses in high-density magnetic recording systems (*36*) and in scanning surface microscopies (*37*). In these areas, there is a well-defined need, the potential impact is high, and developments are proceeding rapidly. Scanning surface microscopy (primarily tunneling and force) promises to revolutionize the field of surface science, and the use of solid-state fabrication techniques to fabricate the critical scan tips is being pursued by several groups. A multichannel probe under development at the University of Michigan (*38*) combines bulk micromachining (for the substrate) with surface micromachining (for the cantilever beams) and uses dry etching for the formation of the stylus tips (Fig. 9). This combined use of the various micromachining processes will probably be widely used in the future as designs capitalize on the best features of each process. Finally, from a business perspective, important and practical new applications for microsystems must be defined in new emerging industries, while in more established industries we must overcome the inertia and real costs associated with moving to this new technology. Although there is no question that system-related sensor features are valuable, the host system level must be willing to change to permit their inclusion. In some cases, entirely new control architectures will be required.

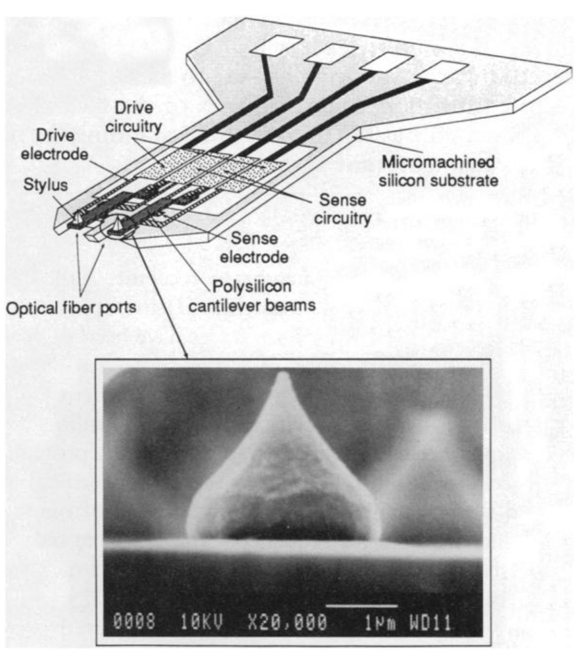

Fig. 9. Structure of a micromachined multichannel atomic force microscope under development at the University of Michigan. The device features a combination of surface and bulk micromachining, with dry etching used to form the iridium-coated polysilicon stylus tips shown. Optical fiber ports are used for optical readout; sense circuitry is for electronic readout.

Conclusions

Significant progress has been made in the ability to fabricate microstructures, sensors, interface circuits, and microactuators with reproducible batch-silicon process technologies. Devices for the measurement of pressure, acceleration, flow, and other variables are now in volume production, and a series of improvements in range, accuracy, cost, and reliability should emerge during the coming decade. Many of these devices will themselves become microsystems, sensing many different parameters and using microactuators to improve performance. For areas where the object of interest is itself small, entire instruments could be reduced to chip proportions.

In this continuing evolution, there are many technical challenges that must be solved. Nonplanar technologies for microsystems are badly needed along with assembly techniques at the submillimeter and micrometer levels. Workstation-based design systems are needed along with databases of material, structural, and performance information that do not now exist. Improved packaging approaches are also needed for most of these systems. The devices with which we are concerned hold the potential of creating the most significant changes in instrumentation and control systems since the development of the microprocessor, and the leveraged impact on the microelectronics industry itself could be similar to that event. Beyond microelectronics, the information gained about important application areas for the technology (such as neural networks and neuroscience) is likely far greater than we can imagine.

REFERENCES AND NOTES

1. K. D. Wise and N. Najafi, *Digest IEEE Int. Conf. Solid-State Sensors Actuators* (June 1991), p. 2.
2. M. P. Lepselter, *Bell System Tech. J.* **45**, 233 (February 1966).
3. R. M. Finne and D. L. Klein, *J. Electrochem. Soc.* **114**, 965 (September 1967).
4. K. E. Petersen, *Proc. IEEE* **70**, 420 (May 1982).
5. C. H. Ozdemir and J. G. Smith, *Digest IEEE Int. Conf. Solid-State Sensors Actuators* (June 1991), p. 132.
6. E. Yoon and K. D. Wise, *Digest 1990 IEEE Solid-State Sensor and Actuator Workshop* (June 1990), p. 161.
7. H. L. Chau and K. D. Wise, *IEEE Trans. Electron Devices* **35**, 2355 (December 1988).
8. R. T. Howe, *J. Vac. Sci. Technol. B* **6**, 1809 (December 1988).
9. K. Najafi, K. D. Wise, T. Mochizuki, *IEEE Trans. Electron Devices* **32**, 1206 (July 1985).
10. K. L. Drake, K. D. Wise, J. Farraye, D. J. Anderson, S. L. BeMent, *IEEE Trans. Biomed. Eng.* **35**, 719 (September 1988).
11. J. Ji and K. D. Wise, *Digest 1990 IEEE Solid-State Sensor Actuator Workshop* (June 1990), p. 107.
12. J. F. Hetke, K. Najafi, K. D. Wise, *Sensors Actuators A* **23**, 999 (April 1990).
13. A. C. Hoogerwerf and K. D. Wise, *Digest IEEE Int. Conf. Solid-State Sensors Actuators* (June 1991), p. 120.
14. A. Hanneborg, *Digest IEEE Workshop MicroElectroMechanical Systems* (January 1991), p. 92.
15. L. J. Spangler and K. D. Wise, *Sensors Actuators A* **24**, 117 (July 1990).
16. J. B. Lasky, S. R. Stiffler, F. R. White, J. R. Abernathey, *Digest IEEE Int. Electron Devices Meeting* (December 1985), p. 684.
17. S. T. Cho, K. Najafi, C. Lowman, K. D. Wise, *ibid.*, p. 499.
18. S. T. Cho and K. D. Wise, *Digest IEEE Int. Conf. Solid-State Sensors Actuators* (June 1991), p. 400.
19. K. Ikeda *et al.*, *Sensors Actuators A* **21**, 146 (February 1990).
20. H. C. Nathanson, W. E. Newell, R. A. Wickstrom, J. R. Davis, *IEEE Trans. Electron Devices* **14**, 117 (March 1967).
21. R. T. Howe and R. S. Muller, *ibid.* **33**, 499 (April 1986).
22. H. Guckel and D. W. Burns, *Digest IEEE Int. Electron Devices Meeting* (December 1984).
23. M. Mehregany, K. J. Gabriel, W. S. N. Trimmer, *IEEE Trans. Electron Devices* **35**, 719 (June 1988).
24. M. Mehregany *et al.*, *Sensors Actuators A* **21–23**, 173 (1990).
25. L. S. Fan, Y. C. Tai, R. S. Muller, *IEEE Trans. Electron Devices* **35**, 724 (June 1988).

26. L. Y. Chen and N. C. MacDonald, *Digest IEEE Int. Conf. Solid-State Sensors Actuators* (June 1991), p. 739.
27. Z. L. Zhang and N. C. MacDonald, *ibid.*, p. 520.
28. Y. Gianchandani and K. Najafi, *Digest IEEE Int. Electron Devices Meeting* (December 1991), in press.
29. K. Suzuki, *ibid.*, p. 625.
30. W. Ehrfeld, F. Gotz, D. Munchmeyer, W. Schelb, D. Schmidt, *Digest IEEE Solid-State Sensor Actuator Workshop* (June 1988), p. 1.
31. H. Guckel *et al.*, *Digest IEEE Solid-State Sensor Actuator Workshop* (June 1990), p. 118.
32. H. Guckel *et al.*, *Digest IEEE Int. Conf. Solid-State Sensors Actuators* (June 1991).
33. Y. W. Kim and M. G. Allen, *ibid.*, p. 651.
34. R. M. Harris, F. Maseeh, S. D. Senturia, *Digest IEEE Solid-State Sensor Workshop* (June 1990), p. 36.
35. Y. Zhang, S. B. Crary, K. D. Wise, *ibid.*, p. 32.
36. H. H. Zappe, *Digest IEEE MicroElectroMechanical Systems* (February 1990).
37. C. F. Quate, *ibid.*, p. 188.
38. L. C. Kong, B. G. Orr, K. D. Wise, *Digest 1990 IEEE Solid-State Sensor Actuator Workshop* (June 1990), p. 28.
39. We acknowledge the many efforts of those at the University of Michigan who have contributed to the work described in this article. In particular, we thank J. Ji, S. Cho, E. Yoon, S. Crary, B. G. Orr, J. F. Hetke, L. C. Kong, N. Najafi, A. C. Hoogerwerf, Y. Gianchandani, and the staff of the Solid-State Fabrication Facility. The support and assistance of F. T. Hambrecht and W. Heetderks of the Neural Prosthesis Program, National Institute of Neurological Disorders and Stroke, R. M. Burger and N. Foster of the Semiconductor Research Corporation, and G. Hazelrigg of the National Science Foundation have made our particular activities at the University of Michigan possible.

Research Article

Three-Dimensional Structures of the Ligand-Binding Domain of the Bacterial Aspartate Receptor With and Without a Ligand

MICHAEL V. MILBURN,* GILBERT G. PRIVÉ,† DANIEL L. MILLIGAN,‡ WILLIAM G. SCOTT, JOANNE YEH, JARMILA JANCARIK, DANIEL E. KOSHLAND, JR.,§ SUNG-HOU KIM§

The three-dimensional structure of an active, disulfide cross-linked dimer of the ligand-binding domain of the *Salmonella typhimurium* aspartate receptor and that of an aspartate complex have been determined by x-ray crystallographic methods at 2.4 and 2.0 angstrom (Å) resolution, respectively. A single subunit is a four–α-helix bundle with two long amino-terminal and carboxyl-terminal helices and two shorter helices that form a cylinder 20 Å in diameter and more than 70 Å long. The two subunits in the disulfide-bonded dimer are related by a crystallographic twofold axis in the apo structure, but by a noncrystallographic twofold axis in the aspartate complex structure. The latter structure reveals that the ligand binding site is located more than 60 Å from the presumed membrane surface and is at the interface of the two subunits. Aspartate binds between two α helices from one subunit and one α helix from the other in a highly charged pocket formed by three arginines. The comparison of the apo and aspartate complex structures shows only small structural changes in the individual subunits, except for one loop region that is disordered, but the subunits appear to change orientation relative to each other. The structures of the two forms of this protein provide a step toward understanding the mechanisms of transmembrane signaling.

TRANSMEMBRANE RECEPTORS ARE THE PROTEINS THROUGH which cells and organisms commonly receive information from the outside of a cell and transmit it for processing inside the cell. One type of receptor is connected to an ion channel and allows a burst of ions to enter or leave the cell, but in most cases the receptor information is probably transferred from exterior to interior through conformational changes in the protein. The mechanism of information transfer is obscure, in part because it has been difficult to crystallize any transmembrane receptor. Although two membrane proteins, a photoreaction center (*1*) and a porin (*2*), have been crystallized and their crystal structures have been determined, they do not have the structure of a typical receptor of signal transduction. For one such class, of which the epidermal growth factor (*3*), platelet-derived growth factor (*4*), insulin (*5*), and low-density lipoprotein (*6*) receptors are typical, the proteins contain an extracellular ligand-binding domain, a cytoplasmic signaling domain, and a transmembrane domain composed of one or two transmembrane hydrophobic sequences. The aspartate receptor of chemotaxis falls in this last category (*7*) and is itself a member of a large family of bacterial protein receptors (*8*). The ligand-binding domain of the aspartate receptor has been crystallized in the presence and absence of aspartate. Structural properties have been revealed that represent an initial step toward unraveling the mechanism of transmembrane signaling in this and other related receptors.

The aspartate receptor of *Salmonella typhimurium* has been extensively studied, and the features of its primary structure are summa-

M. V. Milburn, G. G. Privé, W. G. Scott, J. Yeh, J. Jancarik, and S.-H. Kim are in the Department of Chemistry and Lawrence Berkeley Laboratory, University of California, Berkeley, CA 94720. D. L. Milligan and D. E. Koshland, Jr., are in the Department of Biochemistry, University of California, Berkeley, CA 94720.

*Present address: Department of Structural and Biophysical Chemistry, Glaxo Inc., Research Triangle Park, NC 27790.
†Present address: Molecular Biology Institute, University of California, Los Angeles, CA 90024.
‡Present address: Howard Hughes Medical Institute, University of California, San Francisco, CA 94143.
§To whom correspondence should be addressed.